Bose-Einstein condensation in a simple microtrap

S. Schneider,[1] A. Kasper,[1] Ch. vom Hagen,[1] M. Bartenstein,[1] B. Engeser,[1] T. Schumm,[1] I. Bar-Joseph,[2] R. Folman,[1] L. Feenstra,[1,*] and J. Schmiedmayer[1]

[1]*Physikalisches Institut, Universität Heidelberg, Philosophenweg 12, 69120 Heidelberg, Germany*
[2]*Department of Condensed Matter Physics, The Weizmann Institute of Science, Rehovot 76100, Israel*

A Bose-Einstein condensate is created in a simple and robust miniature Ioffe-Pritchard trap, the so-called Z trap. This trap results from the mere combination of a Z-shaped current-carrying wire and a homogeneous bias field. The experimental procedure allows condensation of typically 3×10^5 ^{87}Rb atoms in the $|F=2, m_F =2\rangle$ state close to any mirroring surface, irrespective of the surface structure. Thus it is ideally suited as a simple coherent source for miniature surface traps or for cold atom physics near surfaces.

PACS number(s): 03.67.Lx, 03.75.Be, 32.80.Pj

Bose-Einstein condensates are at the heart of research in quantum optics. Since the first realization [1,2], various methods of creating a condensate have been shown, ranging from large-scale magnetic traps to miniature surface traps [3,4] as well as optical dipole traps [5]. Many fascinating properties of this form of matter have been studied [6–8].

Manipulation of ultracold atoms using surface mounted microstructures, so-called atom chips [9,10], promises accuracy and versatility in manipulating atoms at the quantum level, and perhaps even the implementation of quantum information processing [11]. For a comprehensive review on surface mounted microtraps, see Ref. [10]. One of the main experimental challenges is to realize a simple coherent source of ultracold (ground state) atoms for the experiments, irrespective of the microstructures on the surface.

In this article we report on the creation of a sizable ($\sim 3 \times 10^5$ atoms) Bose-Einstein condensate in a Z-wire trap, which yields a simple, easy to handle, and robust small-scale Ioffe-Pritchard trap [12]. Placing the Z-wire structure behind the atom chip allows us to separate the magnetic trap geometry for the condensation process from the microtraps for further experiments. Such a setup gives complete freedom in design of the microtraps on the atom chip.

The most basic microtrap uses the magnetic field minimum created by superposing the magnetic field of a current in a straight wire on a homogeneous magnetic bias field perpendicular to it [10,13]. The two fields add up to a two-dimensional quadrupole field along the wire, which can guide atoms. The trap depth is given by the homogeneous bias field; the field gradient is inversely proportional to the wire current. Such a geometry lends itself to miniaturization of the wire size using microfabrication techniques. In this way traps can be made even steeper, while maintaining mechanical stability and robustness. A typical example is our atom chip [9], where the $1-200~\mu$m wide wires are microfabricated in a $2-5~\mu$m thick gold layer on a silicon substrate.

By bending the ends of the wire one creates slightly more complex structures [12,14,15] that provide a three-dimensional confinement (see the inset in Fig. 1).

(a) The U trap: By bending a wire in a U shape, the two fields from the bent ends of the wire (arms) close the initial two-dimensional confinement (guide) along the central wire segment (base). The result is a three-dimensional quadrupole field, with a trap minimum $B_0 = 0$.
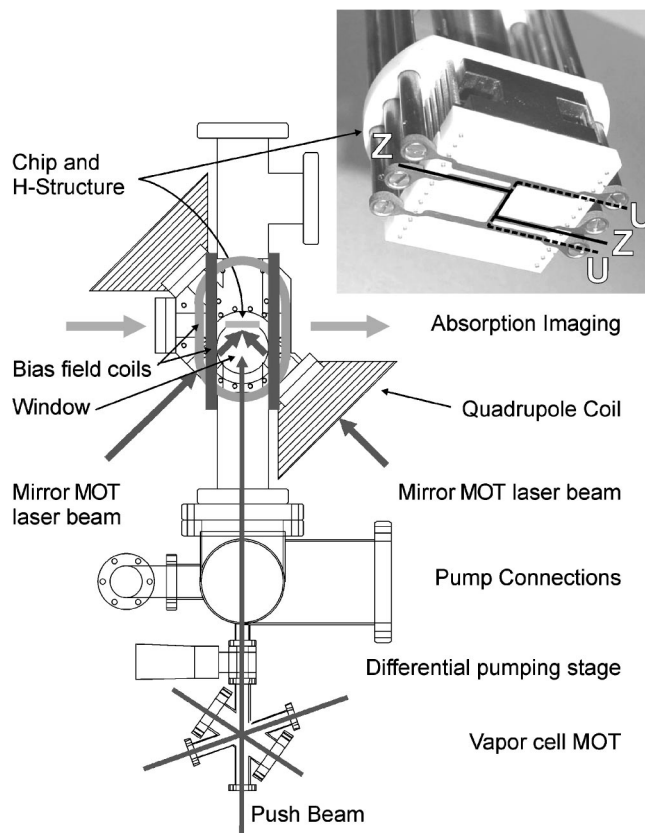

FIG. 1. Scheme of the experimental setup, showing the vacuum chamber, the quadrupole coils, and the 45° laser beams for the mirror-magneto-optical trap (MOT) (see text). The inset shows the copper H structure in the atom chip mounting (seen from below, atom chip not mounted). The current paths for the U and the Z trap are indicated.

*Author to whom correspondence should be addressed. Electronic address: Feenstra@physi.uni-heidelberg.de
URL: http://www.bec.uni-hd.de

(b) The Z trap: If the arms are pointing in opposite directions (Z-shaped wire) a field component parallel to the base remains, giving a Ioffe-Pritchard type trap with a nonzero minimum $B_0 > 0$.

A common property of these traps is the scaling of the strong linear confinement in the transverse direction, inversely proportional to the wire current I_W and the distance z_0 between the wire center and the trap minimum:

$$z_0 \propto \frac{I_W}{B_x}, \quad B'_\perp = \frac{\partial B}{\partial x, z} \propto \frac{B_x^2}{I_W}. \quad (1)$$

Here B_x is the homogeneous bias field perpendicular to the wire. In the case of a Z trap, the additional longitudinal field arising from the arms turns the bottom of the quadrupole trap into a harmonic potential. The transverse angular trap frequencies $\omega_{x,z}$ in this potential scale as

$$\omega_{x,z} \propto \frac{B'_\perp}{\sqrt{B_0}}. \quad (2)$$

Such wire traps provide a linear field gradient given by Eq. (1). This enables a large flexibility first to trap a large number of atoms and second to efficiently compress the trap to small volumes and high trap frequencies for effective evaporative cooling. For instance, using a wire current of $I_W = 50$ A and properly tuned bias fields, thermal atoms can be trapped up to 3 mm from the wire center. By varying only the bias fields, the trap can be compressed to field gradients in excess of 400 G/cm at a trap distance of 1.5 mm from the wire center, reaching trap frequencies of $\omega_{x,z} > 600$ Hz. The large distance allows a microfabricated structure to be placed between the wire and the trap. This is the principal advantage of the experimental setup. An additional benefit of such small-scale circuits is that their low inductance enables rapid changing and switching of the potentials.

As presented in Fig. 1, the experimental apparatus mainly consists of a vertically aligned double magneto-optical trap (MOT) setup with a mirror MOT [9,15–17] in the upper ultrahigh vacuum (UHV) chamber. The atom chip gold layer serves as the mirror [9]. The magnetic quadrupole field for the MOT is supplied by external coils or by the field of the U trap (U MOT). For the mirror MOT to work, the magnetic axis of the quadrupole must be tilted by 45° with respect to the mirror. To maintain the optical access to the trap the coils are wound in a conical shape. Two counterpropagating laser beams overlap the quadrupole axis, being reflected on the mirror at 45°. Two additional counterpropagating laser beams run horizontally, parallel to the mirror and perpendicular to the plane of the 45°-reflected beams. In the case of the U MOT, the 45° angle of the field axis follows naturally from the geometry of the wire and the bias field; therefore the U MOT can be operated with the same laser beam configuration.

The fields for the Z trap and the U MOT are derived from currents through the adequate ports of a monolithic H-shaped copper structure (see the inset of Fig. 1). The central bar of the H structure forms the base wire of both the U and the Z traps. The base wire length for the U MOT is 12.75 mm

(outer ports), while for the Z trap it is 7.25 mm (inner ports). The device is tightly fitted in an insulating ceramic, allowing any structure to be mounted directly against it. The distance between the center of the base wire and the surface of an atom chip is 1.2 mm. The 1.2×1 mm^2 cross section of the base wire withstands currents of up to 50 A for over a minute without significant heating. Thus it enables trapping of large atom numbers both near and far away from the chip surface, while preserving the ultrahigh vacuum in the upper chamber.

The base of the trap mounting is made from stainless steel tubes welded to a UHV flange, allowing a coolant flow through the mounting. The flange also carries four high-power current feedthroughs for operating the H structure and a 35-pin connector to access the atom chip. The ceramic block containing the H structure is fastened to the stainless steel part of the mounting by a copper rod, acting as a heat sink. The mounting is hung from its flange in the upper, ultrahigh vacuum, chamber of the setup, which is machined from a single piece and is fitted with optical quality windows. The distance between the atom trap center and the closest window is ~ 40 mm.

A regular vapor cell MOT in the lower part of the setup traps $\sim 10^9$ ^{87}Rb atoms from the background gas obtained from a heated Rb-dispenser. A continuous laser beam, the push beam, transfers the atoms through a differential pumping stage and over a 40 cm vertical distance from the vapor cell MOT chamber ($P \sim 10^{-8}$ mbar) to the UHV chamber ($P \sim 10^{-11}$ mbar) [18,19].

The experimental cycle starts by loading the mirror MOT with the push beam for 20 s, resulting in a cloud of 10^9 atoms located ~ 3 mm below the atom chip. Next, the quadrupole field from the mirror MOT is gradually replaced in 300 ms by that of the U MOT. Using a wire current of $I_W = 25.5$ A and bias field of $B_x = 6.5$ G, a field gradient of 14 G/cm is reached. The transfer to the U MOT compresses the cloud and moves it to 2 mm from the surface. During this process we observe no atom losses.

After the U MOT phase, all magnetic fields are switched off for 15 ms to allow optical molasses cooling to ~ 50 μK. It should be noted that the atom chip surface is not a perfect mirror, due to the structures on the chip. However, the diffraction from these edges does not harm in any aspect the functionality of the mirror MOT, nor does it inhibit molasses cooling. Next, a 200 μs optical pumping pulse to the $|F = 2, m_F = 2\rangle$ state prepares the atoms for the transfer to the Z trap. Optical pumping increases the number of trapped atoms by a factor of 3. With careful matching of the trap parameters, more than 10^8 atoms can be loaded into the magnetic trap.

The trap frequencies for the initial Z trap, with a Z current of 49.7 A and a bias field of $B_x = 25.4$ G (dotted line in Fig. 2), are $\omega_y = 2\pi \times 18$ Hz and $\omega_{x,z} = 2\pi \times 51$ Hz. Immediately after loading, the offset field of the Z trap is reduced by the addition of a bias field B_y, parallel to the base, opposing the fields of the arms. This compresses the trap transversely and deepens it. After 100 ms this bias field reaches its final value of $B_y = 5.5$ G (dashed line in Fig. 2). The trap is further compressed in all three directions by linearly increasing the bias field B_x from 25.4 G to 58.3 G, which also moves the
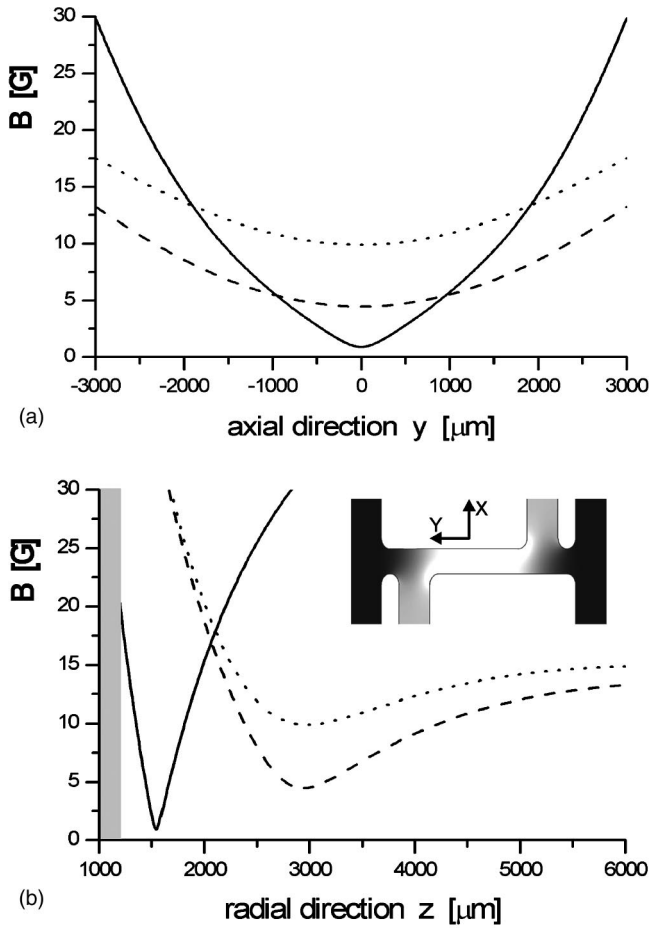
FIG. 3. Absorption image of a compressed atom cloud ($T \sim 10~\mu$K, $N \sim 5 \times 10^5$) $\sim 35~\mu$m away from the atom chip surface. The angle of the imaging laser is adjusted so that the lower image is the direct shadow of the cloud in the beam reflected off the chip. The upper image is due to the part of the beam that strikes the atom cloud before being reflected. The lower panel shows an exaggerated scheme of the setup (actual angle $\sim 0.3°$, picture width 1.8 mm).

FIG. 2. Potentials of the Z trap with $I_W = 49.7$ A for different bias field configurations used in the experiment. Initial trap (dotted line), $B_x = 25.4$ G, $B_y = 0$; compressed trap (dashed line), $B_x = 25.4$ G, $B_y = 5.5$ G; final trap (solid line), $B_x = 58.3$ G, $B_y = 5.5$ G. On the left axis of the lower panel the chip is indicated (surface at $z = 1200~\mu$m). The effect of gravity, along the positive Z direction, is taken into account in the model. The inset in (b) shows the current density in the H structure when used for the Z trap; a lighter shade corresponds to a higher current density.

trap center from initially 1.8 mm to a distance of 300 μm from the chip surface (solid line in Fig. 2). During the 19 s compression stage, forced evaporative cooling is applied by rf radiation from a coil antenna outside the vacuum chamber. The frequency is linearly ramped down from 19 MHz to typically 600 kHz. The simultaneous processes of compression and cooling avoid crushing the initially large atom cloud into the chip surface. For the final trapping potential, the angular oscillation frequencies are $\omega_{x,z} = 2\pi \times 600$ Hz and $\omega_y = 2\pi \times 70$ Hz (solid line in Fig. 2). The compression increases the transverse field gradient by more than a factor of 5, from 80 G/cm to 440 G/cm. The wire current is kept constant throughout the procedure.

The atom cloud is studied by absorption imaging with a weak (120 μW/cm^2) circularly polarized laser beam, resonant with the $F = 2 \rightarrow F' = 3$ transition. The imaging system uses an eight-bit charge-coupled device camera and achromatic optics with a r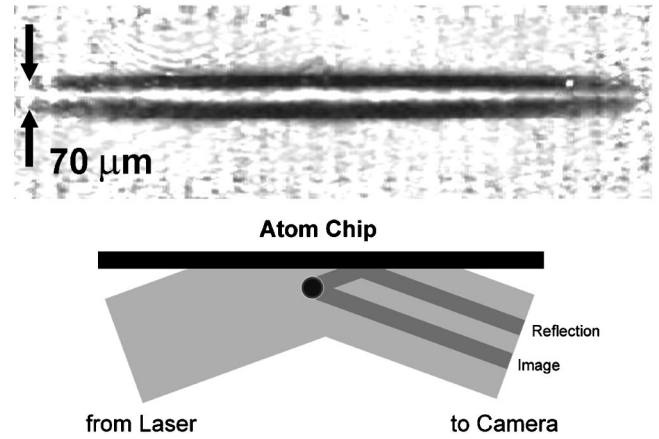esolution of 3 μm. The direction of view is parallel to the plane of the atom chip and perpendicular to the central bar of the H structure. The laser beam grazes the chip, enabling detailed pictures down to very short distances to the chip. Care has to be taken in aligning the absorption laser beam, because slight misalignment can cause severe diffraction stripes to appear in the images.

A helpful feature of the setup is that the distance of the cloud to the chip surface may be inferred from slightly tilting the imaging laser beam; one observes two images of the condensate, where one results from a partially reflected absorption beam (see Fig. 3).

Modeling the trap geometry with a straightforward approach using infinitely long arms and infinitely thin wires, neglecting the finite size of the structure, gives a qualitative estimate for the parameters of the trap. Detailed simulations of the current distribution in the Z structure, employing finite element algorithms, reveal that the effective current path length L_{eff} in the Z structure is shorter than the geometrical value L_{geom} defined by the separation of the arms along the base wire (see the inset in Fig. 2). Using an effective base
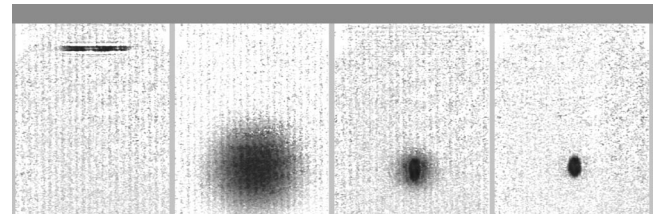

FIG. 4. Bose-Einstein condensation is observed in absorption images taken at different final RF-frequencies ν_f. From left to right: atoms in the trap, $\nu_f = 800$ kHz, expanded clouds after 16 ms time-of-flight with $\nu_f = 800$ kHz (thermal cloud), $\nu_f = 650$ kHz (bimodal cloud), and $\nu_f = 630$ kHz (pure BEC), respectively. Each image size is $\sim 1.8 \times 2.3$ mm. The surface of the atom chip is indicated at the top of the figure.

length of $L_{\text{eff}} \sim 6.7$ mm, instead of $L_{\text{geom}} = 7.25$ mm, in the model with infinitely thin wires, we reach good quantitative agreement with the experimental results.

The procedure described above results in a Bose-Einstein condensate of approximately 3×10^5 atoms, at a density of 9×10^{13} cm^{-3} and with a transition temperature of ~ 600 nK (see Fig. 4).

Presently, the condensate in the copper structure survives for over a second when using rf shielding at the final frequency of the cooling ramp. In addition, we can transfer the condensate to a trap on the atom chip in typically 100 ms.

Since in this work the atom chip is only used as a reflecting surface for the mirror MOT, we have shown that a single current-carrying wire in a homogeneous bias field suffices to create and store a Bose-Einstein condensate near a hot reflective surface, irrespective of its structure. This makes the setup very well suited for studying the interaction between degenerate atom clouds and surfaces. Since the large volume of the macroscopic Z trap allows trapping, storing, and cooling of large atom numbers, the technique can easily be used to load precooled ensembles into small-scale traps of a different nature, such as miniature optical traps, traps made of permanent magnets, electric traps, etc., which may have shallow depths or small trapping volumes, thus lacking the ability to store a sufficient number of atoms for compression and evaporative cooling.

[1] M. Anderson, J. Ensher, M. Matthews, C. Wieman, and E. Cornell, Science **269**, 198 (1995).

[2] K. Davis, M. Mewes, M. Andrews, N.J. van Druten, D. Durfee, D. Kurn, and W. Ketterle, Phys. Rev. Lett. **75**, 3969 (1995).

[3] H. Ott, J. Fortagh, G. Schlotterbeck, A. Grossmann, and C. Zimmermann, Phys. Rev. Lett. **87**, 230401 (2001).

[4] W. Hänsel, P. Hommelhoff, T. Hänsch, and J. Reichel, Nature (London) **413**, 498 (2001).

[5] M. Barrett, J. Sauer, and M. Chapman, Phys. Rev. Lett. **87**, 010404 (2001).

[6] W. Ketterle, D. Durfee, and D. Stamper-Kurn, in *Bose-Einstein Condensation in Atomic Gases*, Proceedings of the International School of Physics "Enrico Fermi," Course CXL, Vavenna, 1998, edited by M. Inguscio (IOS, Amsterdam, 1999), p. 67.

[7] K. Ziemelis, Nature (London) **416**, 205 (2002).

[8] A regularly updated overview of literature on Bose-Einstein condensation can be found at http://amo.phy.gasou.edu/bec.html.

[9] R. Folman, P. Krüger, D. Cassettari, B. Hessmo, T. Maier, and J. Schmiedmayer, Phys. Rev. Lett. **84**, 4749 (2000).

[10] R. Folman, P. Krüger, J. Denschlag, C. Henkel, and J. Schmiedmayer, Adv. At., Mol. Opt. Phys. **48**, 263 (2002).

[11] J. Schmiedmayer, R. Folman, and T. Calarco, J. Mod. Opt. **49**, 1375 (2002).

[12] A. Haase, D. Cassettari, B. Hessmo, and J. Schmiedmayer, Phys. Rev. A **64**, 043405 (2001); A. Haase, Diploma thesis, Freie Universität Berlin, 2000.

[13] R. Frisch and E. Segre, Z. Phys. **75**, 610 (1933).

[14] J. Denschlag, D. Cassettari, A. Chenet, S. Schneider, and J. Schmiedmayer, Appl. Phys. B: Lasers Opt. **69**, 291 (1999).

[15] J. Reichel, W. Hänsel, and T.W. Hänsch, Phys. Rev. Lett. **83**, 3398 (1999).

[16] K. Lee, J. Kim, H. Noh, and W. Jhe, Opt. Lett. **21**, 1177 (1996).

[17] T. Pfau and J. Mlynek, in *Proceedings of the European Quantum Electronics Conference,* edited by K. Burnett (Optical Society of America, Washington, D.C., 1996), p. 33.

[18] M. Bartenstein, Diploma thesis, Freie Universität Berlin, 2001.

[19] W. Wohlleben, F. Chevy, K. Madison, and J. Dalibard, Eur. Phys. J. D **15**, 237 (2001).